

Go With the Flow: Energy Minimising Periodic Trajectories for UVMS

Wilhelm J. Marais¹, Stefan B. Williams¹, Oscar Pizarro¹

Abstract—For Underwater Vehicle Manipulator Systems (UVMS), the ability to keep a fixed end effector pose is required for intervention tasks. Maintaining a static configuration in a dynamic underwater environments requires significant amounts of energy over time, limiting the operational time for battery powered systems. In this work we consider learning the periodic components of the dynamic flow in order to generate periodic trajectories which keep the end effector fixed, yet minimise the energy expenditure over time. We compare this proposed ‘go with the flow’ approach to the static configuration case for a fixed end effector pose, and show a significant reduction in energy use.

I. INTRODUCTION

For an underwater vehicle manipulator system (UVMS), effective operation relies on the ability to maintain a desired end effector pose. These systems contain more Degrees Of Freedom (DOF) than the dimension of the end effector task space, a situation defined as kinematic redundancy. Numerical methods are typically required to solve inverse kinematics problems for these systems [1], yet the additional DOF enable flexibility in choosing between any number of configurations which achieve a given pose [2]. The use of kinematic redundancy to achieve inverse kinematic solutions which have additional desirable properties has been explored in many contexts [3], [4].

The problem of choosing from the infinite set of configurations which achieve a given end effector pose is known as redundancy resolution. Local redundancy resolution methods are generally solved using least squares [5], [6] or quadratic programming methods [7], yet may lead to numerical instabilities and sub-optimal trajectories [8]. Global approaches to redundancy resolution consider longer term trajectories, and initial work used Pontryagin’s maximum principle to derive 2-point boundary value problems [9]. Due to computation difficulties, especially when considering inequality constraints, these methods have been restricted to use in systems with low degrees of redundancy. Recent methods have looked at Model Predictive Control (MPC) for solving redundancy resolution over finite horizons [10], [11]. These methods efficiently handle inequality constraints and are applicable to real-time implementation, yet strict inverse kinematics constraints remain difficult to incorporate.

In underwater environments, disturbances due to the flow of the surrounding water requires active effort from vehicle actuators to counteract [12]. Small to medium sized UVMS

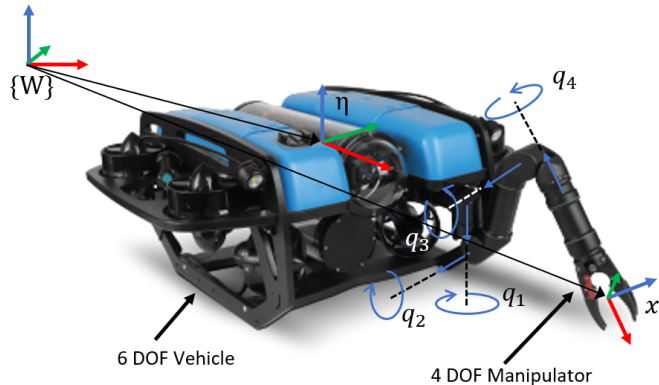


Fig. 1. UVMS used in experiments with a 6 DOF Bluerov vehicle and 4 DOF Blueprint Lab Reach manipulator, showing vehicle pose η and end effector pose x relative to the world frame $\{W\}$. Manipulator joints are labelled q_1 to q_4

and fully autonomous underwater vehicles are generally battery powered, and hence energy use over time is of key consideration [13]. The flow usually contains significant periodic components in shallow waters, and it has been shown in previous work [14] that the details of these periodic disturbances, namely the amplitude, frequency and phase, can be learned. Generally the vehicle has a larger effective area and is affected to a greater extent by the surrounding flow than the manipulator. Therefore keeping the end effector fixed by maintaining a static vehicle pose requires a large amount of energy over time.

Several methods have been proposed for control of underwater vehicles which consider periodic disturbances. MPC with incorporated knowledge of wave disturbances has been used to minimise tracking errors for an underwater vehicle [15] and for UVMS to reduce end effector pose errors due to disturbances [16]. Results show improved performance compared to feedback control methods. Iterative Learning Control (ILC) has been developed as a method which explicitly considers periodic control problems, as well as periodic disturbances, and has seen applications on kinematically redundant manipulators [17].

This paper considers how the kinematic redundancy of the system and knowledge of the flow can be exploited to find trajectories which maintain a fixed end effector pose, while leading to a large reduction in the energy required over time. This involves generating periodic motions which reduce the relative velocity of the vehicle and flow at each timestep, while considering other dynamical effects. Thus the method

¹Authors are with Australian Centre for Field Robotics, University of Sydney, NSW Australia, (j.marais, stefanw, o.pizarro)@acfr.usyd.edu.au

is referred to informally as ‘going with the flow’.

Due to the predictive time horizon method of the approach, it has similarities to MPC style trajectory generation methods, yet few existing approaches consider redundancy resolution over a disturbance period.

This paper makes the following contributions:

- Formulation of a method for online learning of flow velocity components using adaptive oscillators
- Development of an optimisation based approach for generating energy minimising trajectories
- Simulated results showing significant reduction in energy use over time compared to the static configuration case, while keeping the end effector pose fixed
- An example of how an energy minimising trajectory can reduce the end effector pose error when affected by large disturbances
- Analysis of the sensitivity of the proposed method to dynamic modelling errors, showing robustness up to significant amounts of added parameter noise

The remainder of the paper is structured as follows. Section II describes the existing kinematic and dynamic models used to describe UVMS, and how details of the periodic disturbances can be learned online. Section III gives a definition of redundancy parameterisation, and introduces differential kinematics for parameterised systems. Some simple implementation examples for the proposed method are given. Section IV details the formulation of the energy minimising trajectory as a linearly constrained non-linear optimisation problem. Results of the method are presented in Section V, and finally concluding remarks and future work in Section VI.

II. MODELLING OF UVMS

A. Kinematic Modelling

A vehicle manipulator system has system configuration $\theta = (\eta, q)^T$, with $\dim(\theta) = n$, where $\eta \in SE(3)$ is the vehicle pose in the world frame, and $q \in \mathbb{R}^{n-6}$ is the manipulator joint angles. Given some end effector pose x where $\dim(x) = m$, in the world frame, the forward non-linear map f gives

$$x = f(\theta) \quad (1)$$

In this paper we consider $x \in SE(3)$ with $m = 6$. Figure 1 shows the coordinate frames for the system considered in this work. Differentiating the above relationship gives the differential kinematics relationship

$$\dot{x} = J\dot{\theta} \quad (2)$$

where $J \in \mathbb{R}^{m \times n}$, and $\dot{\theta} \in \mathbb{R}^n$ describes the system velocities in the vehicle frame, and $\dot{x} \in \mathbb{R}^m$ is the end effector velocities in the world frame. Note that this work considers fully actuated holonomic systems.

B. Dynamic Modelling

The dynamics of the system are given by [18]

$$M(\theta)\ddot{\theta} + C(\theta, \dot{\theta})\dot{\theta} + D(\theta, \dot{\theta}, \dot{v}_v)(\dot{\theta} - v_v) + g(\theta) = Bu \quad (3)$$

where $M(\theta)$ is the configuration dependent mass matrix, $C(\theta, \dot{\theta})$ is the vector of Coriolis forces, $g(\theta)$ is the vector of gravity (and buoyancy) forces, u is the effort of each actuator, and B is a mapping from u to the force/torque of each DOF. Finally $D(\theta, \dot{\theta}, v_v)$ is the vector of damping terms, which can be expanded as

$$D(\theta, \dot{\theta}, v_v) = D_L(\theta) + D_Q(\theta, |\dot{\theta} - v_v|) \quad (4)$$

where D_L and D_Q are diagonal matrices of linear and quadratic drag terms. Finally $v_v = J_R(\theta)v_d$, where v_v is the velocity of the surrounding flow relative to the world frame given in the vehicle frame, v_d is the flow given in the world frame, and $J_R(\theta)$ is the transformation from the world frame to the vehicle frame. Therefore $(\dot{\theta} - v_v)$ is the relative velocity of the vehicle and the surrounding fluid, expressed in the vehicle frame.

Expansion of other terms in Equation 3 gives

$$M(\theta) = M_i(\theta) + M_a(\theta) \quad (5)$$

$$C(\theta, \dot{\theta}) = C_i(\theta, \dot{\theta}) + C_a(\theta, \dot{\theta}) \quad (6)$$

In Equations 5 and 6, M_i , M_a , C_i and C_a are the inertial and added mass matrices, and inertial and added Coriolis matrices respectively.

C. Estimating Hydrodynamic Parameters

Inertial and hydrostatic parameters such as mass, moment of inertia and buoyancy are relatively easy to determine either from static measurements or 3D models. Hydrodynamic parameters are harder to estimate, and have to be determined experimentally. This section details how these parameters can be estimated in a zero flow environment. Accurate knowledge of hydrodynamic parameters is required for estimation of the periodic flow characteristics. Standard linear regression models can be used for hydrodynamic parameter estimation for underwater vehicles [19]. This method uses a linear observation model

$$H\pi = y \quad (7)$$

where H is the regressor matrix, π is the vector of parameters to be estimated, and y is the observation vector. Assuming simplifications due to symmetry and low relative velocities [18], each unknown in π contains 6 terms, for a total of 18 unknowns for each rigid body. Now Equation 7 can be solved as a linear least squares problem with linear constraints to enforce positive drag and added mass terms.

$$\min_{\pi} \|y - H\pi\|^2, \pi \geq 0 \quad (8)$$

D. Online Learning of Periodic Flows

Assuming good prior estimates of all dynamic parameters from above, the observed dynamic response of the system can be used to learn the period, phase and amplitude of the disturbance signal. This is run online since the flow parameters are not static over time. Adaptive Frequency Oscillators (AFO) are commonly used to learn periodic signals [20], and have

seen applications in several robotics applications [21], [14]. In this paper the estimated periodic flow velocity is modelled by

$$\hat{v}_d = \sum_{i=1}^K \hat{\alpha}_i \sin(\hat{\omega}_i t + \hat{\phi}_i) \quad (9)$$

where $\hat{\alpha}_i$, $\hat{\omega}_i$ and $\hat{\phi}_i$ are the amplitude, frequency and phase respectively of the i th frequency component, and K is the total number of frequency components in the learned signal \hat{v}_d . Using the dispersion relation for the wave frequencies and water depths considered in this work, the wavelength is found to be on the order of 50 metres. This wavelength is around 2 orders of magnitude larger than the motion trajectory of the vehicle and position dependence of the wave velocity can therefore be ignored. The following adaptive integrators are used based on [20]

$$\dot{\hat{\omega}}_i(t) = \nu F(t) \cos(\hat{\phi}_i(t)) \quad (10)$$

$$\dot{\hat{\phi}}_i(t) = \hat{\omega}_i(t) + \nu F(t) \cos(\hat{\phi}_i(t)) \quad (11)$$

$$\dot{\hat{\alpha}}_i(t) = \eta F(t) \sin(\hat{\phi}_i(t)) \quad (12)$$

where F is the driving signal. In this work there is not a direct signal to be learned, but rather the flow velocity has to be estimated from observing the dynamics of the system. Using the observed difference in acceleration as $F = J_r^{-1} M(\ddot{\theta} - \hat{\ddot{\theta}})$ where

$$M\ddot{\theta} = Bu - C\dot{\theta} - D(\dot{\theta} - v_v) - g_k \quad (13)$$

$$M\hat{\ddot{\theta}} = Bu - C\dot{\theta} - \hat{D}(\dot{\theta} - \hat{v}_v) - g_k \quad (14)$$

which simplifies to

$$M(\ddot{\theta} - \hat{\ddot{\theta}}) = D(v_v - \dot{\theta}) - \hat{D}(\hat{v}_v - \dot{\theta}) \quad (15)$$

Note $\hat{v}_v = J_r \hat{v}_d$, which is the estimated flow velocity in the vehicle frame, and J_r^{-1} is the transform from the the vehicle frame to the world frame in which the flow is estimated.

III. REDUNDANCY PARAMETERISATION

A. Definition

Kinematic redundancy occurs when $n > m$, which gives $\theta_r \subset \theta$, where $\dim(\theta_r) = (n - m)$, which is the space of configurations which satisfy Equation 1 for a given x . We therefore have an infinite number of solutions to Equation 1, which can be exploited to find configurations which optimise some secondary objective. Null space projection methods [5] have been proposed for redundancy resolution. This involves projecting the gradient of a secondary objective onto the set of null velocities of the system. The projection matrix is given by $(I_n - J^+ J)$, where J^+ is the pseudo-inverse of J . This projective gradient descent method does not effectively search the available space of redundant configurations [22]. Redundancy parameterisation methods have been proposed [22], [23], which explicitly consider the $(n - m)$ dimensional space of redundant configurations. This allows for significant dimension reduction in the secondary objective optimisation

problem. Previous work by the authors [24] has looked at redundancy parameterisation for an UVMS.

Given an appropriate parameterisation, the vector of velocities of the redundant DOF is given by $\dot{\theta}_r \in \mathbb{R}^{n-m}$. For a fixed end effector pose, the relationship between the $\dot{\theta}_r$ and $\dot{\theta}$ is given by

$$\dot{\theta} = A_r(\theta) \dot{\theta}_r, \quad \dot{x} = 0 \quad (16)$$

where $A_r(\theta) \in \mathbb{R}^{n \times (n-m)}$ is the redundant Jacobian **which contains a linearly independent set of basis vectors spanning the null space**, with definition

$$J A_r(\theta) \dot{\theta}_r = 0 \quad (17)$$

The general inverse differential kinematics can be written as

$$\dot{\theta} = J^+ \dot{x} + A_r(\theta) \dot{\theta}_r \quad (18)$$

where J^+ is the pseudoinverse of J .

The primary advantage of redundancy parameterisation is a significant dimension reduction when optimising over the space of kinematic redundancy. This is essential for large optimisation problems such as presented in Section IV. The inverse kinematics is also explicitly satisfied in the redundancy parameterisation framework, removing the need for a non-linear equality constraint when searching through configurations.

IV. ENERGY MINIMISING TRAJECTORY

A. Trajectory Optimisation

We assume we have a learned disturbance signal with period T , and velocity vector $v_v(t)$ in the vehicle frame. Section II-D details the online disturbance learning method.

The aim is to minimise the total energy used over each disturbance period, while keeping the end effector fixed at a desired pose. The actuator effort u can be found from Equation 3 as

$$u = B^+(M\ddot{\theta} + C\dot{\theta} + D(\dot{\theta} - v_v) + g) \quad (19)$$

The power used by each thruster is proportional to $|u|^{3/2}$ [25]. The power used by the manipulator is ignored since in the unloaded state the total power draw is around 5 watts, while the 8 vehicle thrusters draw around 50 watts each. This significantly reduces the complexity of the optimisation since only the rigid body dynamics of the vehicle body have to be computed over a trajectory. Since the manipulator only has 4 DOF, it is unable to fully compensate for vehicle motion even for small disturbances, and therefore trajectories which only require manipulator effort are not possible. Given the thruster power relationship, the problem is formulated as a $L^{1.5}$ minimisation over the trajectory given by

$$\min_{\theta(t)} \int_{t=0}^T |u(t)|^T \Lambda |u(t)|^{0.5} dt \quad (20)$$

with diagonal weighting Λ , where $|u(t)|$ is the element-wise absolute value of $u(t)$ and $|u(t)|^{0.5}$ is the element-wise square-root of the absolute values. In this work all thrusters are

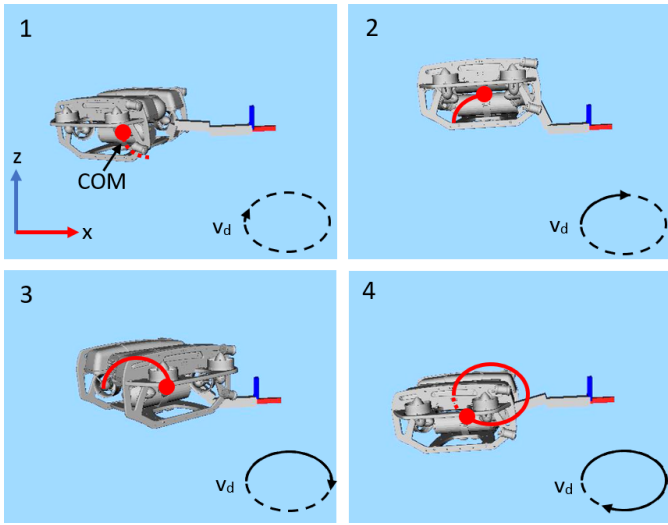


Fig. 4. Image sequence showing energy minimising trajectory for periodic flow in the xz plane, and the motion of the Centre of Mass (COM) of the vehicle

estimated online as per Section II-D. The periodic flow is simulated as shallow water waves, contains only one frequency component, and follows an elliptical path in the xz plane. The periodic learning component assumes one frequency component along each of the 6 (3 translation, 3 rotation) axes ($K = 1$ in Equation 9). Figure 2 shows the estimation of the frequency and amplitude along the x and z directions over time. Figure 3 shows the estimated and true flow velocity over time. The estimated flow velocity closely matches the actual velocity after 3 periods. The amplitude estimation of the other 4 axes remains at 0.

B. Energy Minimising Trajectory

Using the estimated flow velocity from above, an energy minimising trajectory which maintains a fixed end effector pose at a desired setpoint, can be calculated over one flow period. The desired end effector pose setpoint is set to the origin. We compare the trajectory optimised case to the case of a static redundant configuration setpoint. Figure 4 shows an image sequence of the UVMS along the trajectory, showing the motion of the Centre of Mass (COM) of the vehicle, and the flow velocity v_d . The sequence shows the main result of this work, that a ‘go with the flow’ trajectory can minimise energy use, while keeping the end effector pose fixed. The top plot in Figure 5 compares the results of the instantaneous power for the static and trajectory optimised cases, as well as the average power use over time. The total energy use for the static configuration is around 2.5 times that for the optimised trajectory. For the system considered in this work, this would lead to a battery capacity of around 50 minutes vs 130 minutes. The bottom plot of Figure 5 compares the end effector deviation from the desired static pose. The translation and rotational error for the static case are negligible. When following the energy minimising trajectory, the translation error is around 3mm, and maximum rotation error is approximately 0.8° .

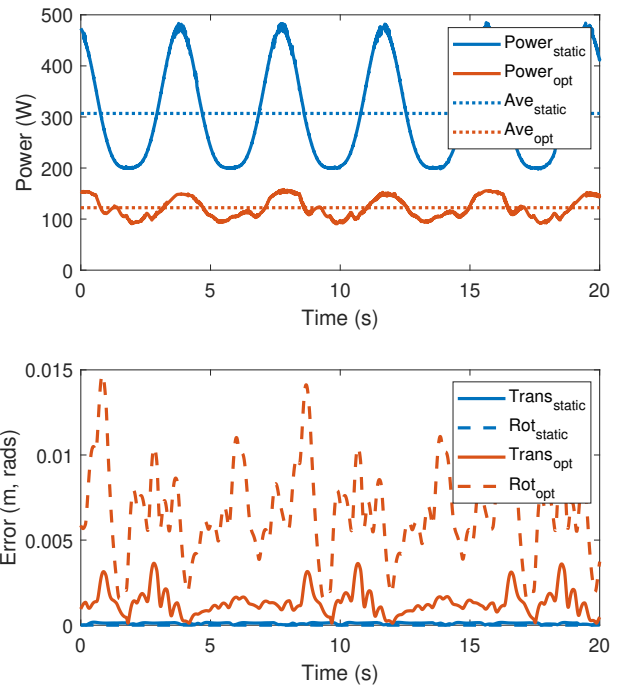


Fig. 5. (top) Comparison of the power use over time for the static and trajectory optimised cases, as well as the total averaged power use, and (bottom) comparison of end effector translational and rotational pose error over the same time period

These values are negligible compared to errors in odometry and flexible strain in the vehicle during operation.

C. Error Minimisation for Large Disturbances

For large disturbances, the system struggles to hold a static configuration due to actuator saturation, resulting in large end effector pose errors. Generating a trajectory which minimises the $L^{1.5}$ norm, also minimises large actuator outputs which limits actuator saturation. The maximum normalised actuator effort is shown in the top plot of Figure 6, with saturation seen as a normalised effort of 1. The bottom plot of Figure 6, shows the corresponding translation and rotation end effector pose errors, which are significant around times of actuator saturation. By generating an energy minimising trajectory, actuator saturation is largely avoided throughout the optimised trajectory, and hence end effector error is also minimised.

D. Sensitivity to Parameter Estimation Error

The previous results assumed perfect knowledge of the hydrodynamic parameters in both the flow estimation and energy minimising trajectory generation stages. In this section we analyse the sensitivity of the proposed methods to errors in hydrodynamic parameter estimation. Normally distributed errors of varying relative standard deviation are added to each of the linear drag, quadratic drag, and added mass terms to determine the effects.

Figure 7 shows the results of learning the velocity waveforms with a 50% relative standard deviation error on the

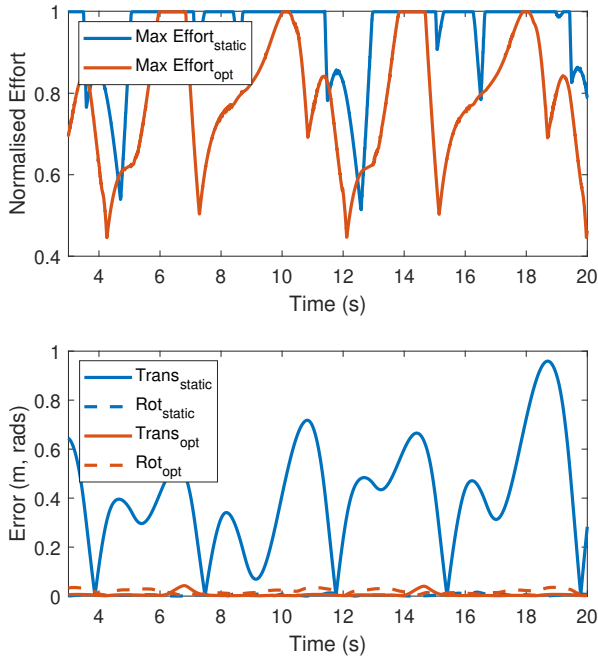


Fig. 6. (top) Comparison of the maximum normalised actuator effort over time for the static and trajectory optimised cases, and (bottom) comparison of end effector translation and rotation pose error over the same time period, for a large flow disturbance

hydrodynamic parameters. The frequency learning converges similarly to the case with no error, yet the amplitudes settle with a steady-state error. Figure 8 shows the results of the amplitude and frequency estimation errors over a range of error magnitudes. The frequency errors remain negligible, yet the amplitude errors grow to around $0.1ms^{-1}$ at 50% error, and $0.24ms^{-1}$ at 100% error. Energy minimising trajectories were calculated using the hydrodynamic parameter and cor-

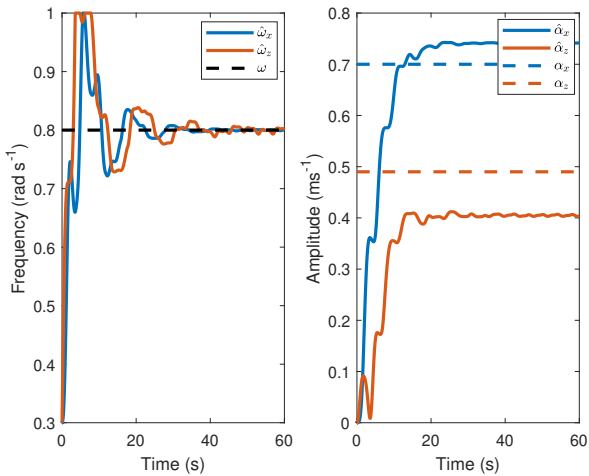


Fig. 7. Learning frequency and amplitude values of periodic flow over time, with 50% relative standard deviation normally distributed errors added to the linear and quadratic drag and added mass terms in the estimated dynamic model

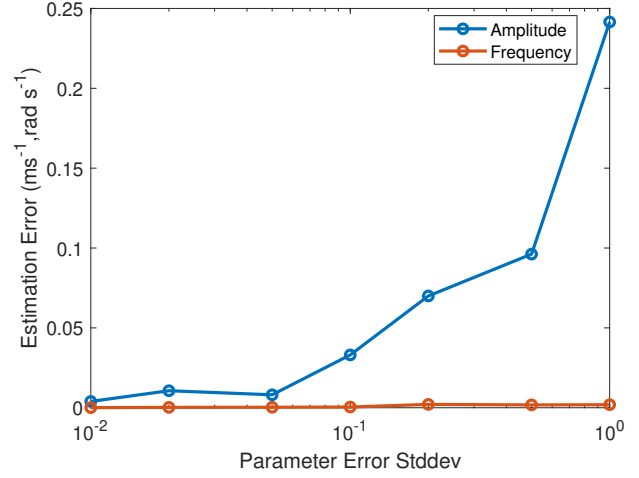


Fig. 8. Periodic flow steady state amplitude and frequency estimation errors vs relative standard deviation of normally distributed hydrodynamic parameter estimation errors

responding waveform estimation errors. The average power use over time for increasing errors is shown in Figure 9. There is a minimal effect on the effectiveness of the proposed energy minimising trajectory method, even at relatively large estimation errors. Since the phase and frequency of the waveform can still be accurately determined, the resulting optimised trajectory still approximately follows the velocity of the surrounding flow to a relative degree, suggesting the method is robust to significant modelling errors.

VI. CONCLUSION

This paper describes methods for generating periodic trajectories for an UVMS in periodic flows, which keep the end effector pose fixed yet minimise the power required. Simulated results show that periodic components of the flow can be learned by driving an adaptive oscillator with the error in the observed dynamics of the system. Further results show that

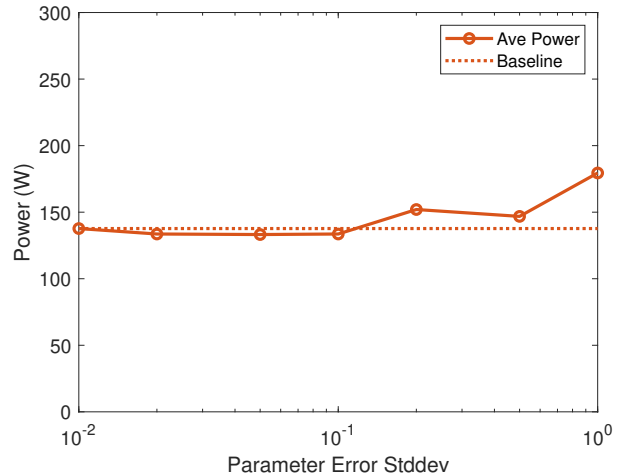


Fig. 9. Average power use over time vs relative standard deviation of normally distributed hydrodynamic parameter estimation errors

tracking energy minimising trajectories lead to significantly reduced power requirements, while keeping the end effector pose relatively stable. Future work aims to look at learning multiple frequency components simultaneously, and adapting the trajectory in real-time. Further work aims for hardware implementation in environments with both controllable and uncontrollable flows.

REFERENCES

- [1] A. Colomé and C. Torras, "Redundant inverse kinematics: Experimental comparative review and two enhancements," in *2012 IEEE/RSJ International Conference on Intelligent Robots and Systems*, 2012, pp. 5333–5340.
- [2] N. Somani, M. Rickert, A. Gaschler, C. Cai, A. Perzylo, and A. Knoll, "Task level robot programming using prioritized non-linear inequality constraints," in *2016 IEEE/RSJ International Conference on Intelligent Robots and Systems (IROS)*, 2016, pp. 430–437.
- [3] N. Jaquier, L. Rozo, D. G. Caldwell, and S. Calinon, "Geometry-aware manipulability learning, tracking, and transfer," *The International Journal of Robotics Research*, vol. 40, no. 2-3, pp. 624–650, 2021, pMID: 33994629. [Online]. Available: <https://doi.org/10.1177/0278364920946815>
- [4] P. Cieslak, P. Ridao, and M. Giergiel, "Autonomous underwater panel operation by girona500 uvm: A practical approach to autonomous underwater manipulation," in *2015 IEEE International Conference on Robotics and Automation (ICRA)*, May 2015, pp. 529–536.
- [5] C. A. Klein and C. Huang, "Review of pseudoinverse control for use with kinematically redundant manipulators," *IEEE Transactions on Systems, Man, and Cybernetics*, vol. SMC-13, no. 2, pp. 245–250, March 1983.
- [6] K. Al Khudir, G. Halvorsen, L. Lanari, and A. De Luca, "Stable torque optimization for redundant robots using a short preview," *IEEE Robotics and Automation Letters*, vol. 4, no. 2, pp. 2046–2053, 2019.
- [7] O. Kanoun, F. Lamiroux, and P.-B. Wieber, "Kinematic control of redundant manipulators: Generalizing the task-priority framework to inequality task," *IEEE Transactions on Robotics*, vol. 27, no. 4, pp. 785–792, 2011.
- [8] K. Kazerounian and Z. Wang, "Global versus local optimization in redundancy resolution of robotic manipulators," *The International Journal of Robotics Research*, vol. 7, no. 5, pp. 3–12, 1988. [Online]. Available: <https://doi.org/10.1177/027836498800700501>
- [9] K. Suh and J. Hollerbach, "Local versus global torque optimization of redundant manipulators," in *Proceedings. 1987 IEEE International Conference on Robotics and Automation*, vol. 4, 1987, pp. 619–624.
- [10] M. Faroni, M. Beschi, L. M. Tosatti, and A. Visioli, "A predictive approach to redundancy resolution for robot manipulators," *IFAC-PapersOnLine*, vol. 50, no. 1, pp. 8975–8980, 2017, 20th IFAC World Congress. [Online]. Available: <https://www.sciencedirect.com/science/article/pii/S2405896317318499>
- [11] D. Lunni, A. Santamaria-Navarro, R. Rossi, P. Rocco, L. Bascetta, and J. Andrade-Cetto, "Nonlinear model predictive control for aerial manipulation," in *2017 International Conference on Unmanned Aircraft Systems (ICUAS)*, 2017, pp. 87–93.
- [12] T. Battista, C. Woolsey, L. McCue-Weil, E. Paterson, and F. Valentinis, "Underwater vehicle depth and attitude regulation in plane progressive waves," in *2015 54th IEEE Conference on Decision and Control (CDC)*, 2015, pp. 4400–4405.
- [13] M. Sarkar, S. Nandy, S. Vadali, S. Roy, and S. Shome, "Modelling and simulation of a robust energy efficient auv controller," *Mathematics and Computers in Simulation*, vol. 121, pp. 34–47, 2016. [Online]. Available: <https://www.sciencedirect.com/science/article/pii/S037847541500186X>
- [14] P. Kormushev and D. G. Caldwell, "Improving the energy efficiency of autonomous underwater vehicles by learning to model disturbances," in *2013 IEEE/RSJ International Conference on Intelligent Robots and Systems*, 2013, pp. 3885–3892.
- [15] D. C. Fernández and G. A. Hollinger, "Model predictive control for underwater robots in ocean waves," *IEEE Robotics and Automation Letters*, vol. 2, no. 1, pp. 88–95, 2017.
- [16] J. Woolfrey, W. Lu, and D. Liu, "Predictive end-effector control of manipulators on moving platforms under disturbance," *IEEE Transactions on Robotics*, pp. 1–8, 2021.
- [17] S. Arimoto, M. Sekimoto, and S. Kawamura, "Task-space iterative learning for redundant robotic systems: Existence of a task-space control and convergence of learning," *SICE Journal of Control, Measurement, and System Integration*, vol. 1, pp. 312–319, 01 2011.
- [18] G. Antonelli, *Underwater Robots: Motion and Force Control of Vehicle-Manipulator Systems*, 2005, vol. 2.
- [19] S. C. Martin and L. L. Whitcomb, "Experimental identification of six-degree-of-freedom coupled dynamic plant models for underwater robot vehicles," *IEEE Journal of Oceanic Engineering*, vol. 39, no. 4, pp. 662–671, 2014.
- [20] L. Righetti, J. Buchli, and A. J. Ijspeert, "Dynamic hebbian learning in adaptive frequency oscillators," *Physica D: Nonlinear Phenomena*, vol. 216, no. 2, pp. 269–281, 2006. [Online]. Available: <https://www.sciencedirect.com/science/article/pii/S0167278906000819>
- [21] K. Seo, K. Kim, Y. J. Park, J.-K. Cho, J. Lee, B. Choi, B. Lim, Y. Lee, and Y. Shim, "Adaptive oscillator-based control for active lower-limb exoskeleton and its metabolic impact," in *2018 IEEE International Conference on Robotics and Automation (ICRA)*, 2018, pp. 6752–6758.
- [22] W. Wiedmeyer, P. Altoé, J. Auberle, C. Ledermann, and T. Kröger, "A real-time-capable closed-form multi-objective redundancy resolution scheme for seven-dof serial manipulators," *IEEE Robotics and Automation Letters*, vol. 6, no. 2, pp. 431–438, 2021.
- [23] D. Busson and R. Béarée, "A pragmatic approach to exploiting full force capacity for serial redundant manipulators," *IEEE Robotics and Automation Letters*, vol. 3, no. 2, pp. 888–894, April 2018.
- [24] W. J. Marais, S. B. Williams, and O. Pizarro, "Anisotropic disturbance rejection for kinematically redundant systems with applications on an uvm," *IEEE Robotics and Automation Letters*, vol. 6, no. 4, pp. 7017–7024, 2021.
- [25] A. J. Healey, S. M. Rock, S. Cody, D. Miles, and J. P. Brown, "Toward an improved understanding of thruster dynamics for underwater vehicles," in *Proceedings of IEEE Symposium on Autonomous Underwater Vehicle Technology (AUV'94)*, July 1994, pp. 340–352.